

# The Effect of Inhomogeneous Broadening on Characteristics of Three-State Lasing InGaAs/GaAs Quantum Dot Lasers

Azam Shafieenezhad, Esfandiar Rajaei ,Saeed Yazdani

Department of physics, University of Guilan, Rasht, Iran

Email : Shafiee.azam1988@gmail.com

**Abstract**—We have investigated the effects of inhomogeneous broadening on the three-state of InGaAs/GaAs quantum dot (QD) lasers. The Numerical models based on rate equations is presented with considering inhomogeneous broadening. We have calculated output power and optical gain that show differences lasing from the ground state and excited state and upper continuum state. The comparison between these three energy levels leads to a qualitative understanding for origin of the three-state lasing in InGaAs/GaAs QD lasers.

**Keywords**— Energy level, inhomogeneous broadening, Output Power, Quantum dot lasers , Rate equations

## I. Introduction

Quantum dot (QD) lasers are promising for uncooled operation due to the 3-D confinement and delta-like density-of-states (DOS) of the QD systems. As such, superior laser characteristics such as low threshold current, high internal efficiency  $\eta_i$  have been demonstrated [i]–[iii]. Semiconductor (QD) lasers also were predicted to offer significant advantages over lasers of higher dimensionality such as bulk, quantum well and wire in terms of spectrum linewidth, modulation bandwidth, temperature stability, and higher optical gain due to the delta function like discrete density of states, that is known as semi-atom. [iv]–[ix]. Experiments and calculations shows high output power can be achieved using lower inhomogeneous broadening and number, there exist an optimum number of QD layers to achieve the highest output power from the device. Here we investigate the influence of homogeneous and specially inhomogeneous broadening on the static and dynamic properties of QD lasers, such as turn on delay and threshold current considering with coverage factor. However, it is conceptual in nature and hence does not include the practical issue of gain broadening. Homogeneous broadening is fundamental while the inhomogeneous broadening [x] characterizes all self assembled QD structures and is known to have an important impact on both static and dynamical properties [x], [xi]. The QDs investigated in this work are InGaAs QDs embedded in a waveguide formed by GaAs/AlGaAs cladding layers. This kind of QD is the most widely investigated QD structure. The effect of inhomogeneous broadening and also homogeneous broadening is an important indicator in QD lasers, Since affecting on output power and optical gain. The model is quite successful in the modeling of lasing spectra [xii], [xiii]. Note that at high bias condition, lasing begins from excited states, therefore, coherent and incoherent

nonlinearities and different scattering mechanism, especially Auger and phonon scattering, govern the lasing action [xiv]. The inhomogeneous broadening was incorporated in the model developed in [xv]. Lots of studies have been done on the simulation of spectral behavior and dynamic characteristics of self-assembled QD lasers [xvi]–[xxi].

In this article, first we explain about transitions between and energy states in laser cavity, then we demonstrate rate equations and mathematical relations and their integrated together. After that we describe numerical results and simulations. Finally we will conclude how inhomogeneous broadening affects on InGaAs/GaAs (QD) lasers.

## II. Material and Methodology

In this section, a numerical model is used to study carrier dynamics in energy levels of an InGaAs/GaAs QD system. In our model, four discrete energy levels, i.e., wetting layer (WL), CS, GS, and ES of each group of QD.

A few similar assumptions are made in the simulation model. Firstly, distribution of QDs is random in each layer of the device structure. Secondly, there is no correlation among different dot layers and thus simplifying the calculation. Thirdly, all carriers in each group of QD ensembles have same relaxation and recombination rates. Lastly, carrier emission from higher dimensional confinement to lower confinement does not change with temperature but depends dominantly on the probability of carrier population. Besides that, a series of longitudinal cavity photon modes are taken into account over the inter-band transition energy of QDs to describe the interaction between the dots with different resonant energies and generated photons. Carrier thermal emission is assumed to occur among three energy levels in QD ensemble and also between CS and WL. The details of carrier population relaxation and reemission dynamics are schematically illustrated in Fig. 1

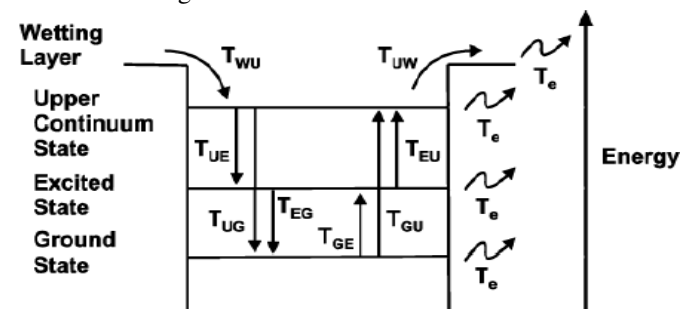


**Fig.1.** Schematic of the energy band diagram that indicates the four different energy levels of wetting layer, upper continuum state, excited state and ground state of each group of QD ensemble with the inclusion of carrier capture and escape lifetime from the various states are shown.

The model follows the set of rate equations described in [xxii] with the additions needed to address the homogeneous and inhomogeneous gain broadening. According Fig.1 the rate equations in our model are as follows:

$$\frac{dN_w}{dt} = \frac{\eta_i I}{e} - \frac{N_w}{T_{wr}} - \frac{N_w}{T_{wuo}} (1 - P_u) - \frac{N_e}{T_e} + \frac{N_u}{T_{uw}} - \frac{N_w}{T_r} \quad (1)$$

$$\begin{aligned} \frac{dN_u}{dt} &= \frac{N_w}{T_{wuo}} (1 - P_u) + \frac{N_g}{T_{gu}} (1 - P_u) \\ &+ \frac{N_e}{T_{eu}} (1 - P_u) - \frac{N_u}{T_{ug}} (1 - P_g) \\ &- \frac{N_u}{T_{ueo}} (1 - P_e) - \frac{N_u}{T_{uw}} - \frac{N_u}{T_e} - \frac{N_u}{T_r} \\ &- \Gamma \nu_g K_u (2P_u - 1) \times \left( \frac{S_u}{1 + \epsilon_{us} S_u} \right) \end{aligned} \quad (2)$$

$$\begin{aligned} \frac{dN_e}{dt} &= \frac{N_u}{T_{ueo}} (1 - P_e) + \frac{N_g}{T_{ge}} (1 - P_e) - \frac{N_e}{T_{eu}} (1 - P_u) - \frac{N_e}{T_{ego}} (1 - P_g) \\ &- \frac{N_e}{T_e} - \frac{N_e}{T_r} - \Gamma \nu_g K_e (2P_e - 1) \times \left( \frac{S_e}{1 + \epsilon_{es} S_e} \right) \end{aligned} \quad (3)$$

$$\begin{aligned} \frac{dN_g}{dt} &= \frac{N_u}{T_{ugo}} (1 - P_g) + \frac{N_e}{T_{ego}} (1 - P_g) - \frac{N_g}{T_{gu}} (1 - P_u) - \frac{N_g}{T_{ge}} (1 - P_e) \\ &- \frac{N_g}{T_e} - \frac{N_g}{T_r} - \Gamma \nu_g K_g (2P_g - 1) \times \left( \frac{S_g}{1 + \epsilon_{gs} S_g} \right) \end{aligned} \quad (4)$$

$$\frac{dS_u}{dt} = \Gamma \nu_g K_u (2P_u - 1) \left( \frac{S_u}{1 + \epsilon_{us} S_u} \right) + \frac{\beta N_u}{T_{sp}} - \frac{S_u}{T_p} \quad (5)$$

$$\frac{dS_e}{dt} = \Gamma \nu_g K_e (2P_e - 1) \left( \frac{S_e}{1 + \epsilon_{es} S_e} \right) + \frac{\beta N_e}{T_{sp}} - \frac{S_e}{T_p} \quad (6)$$

$$\frac{dS_g}{dt} = \Gamma \nu_g K_g (2P_g - 1) \left( \frac{S_g}{1 + \epsilon_{gs} S_g} \right) + \frac{\beta N_g}{T_{sp}} - \frac{S_g}{T_p} \quad (7)$$

The parameters of  $N_w$ ,  $N_u$ ,  $N_e$ ,  $N_g$  refer to total carrier population of wetting layer, carrier population of upper continuum state (CS), excited state (ES) and ground state (GS), respectively. Also  $S_u$ ,  $S_e$ ,  $S_g$  refer to photon density of CS, ES and GS, respectively. For above rate equations, optical gain for CS, ES and GS state can be wrote as follows:

$$g_{cs} = \frac{2\pi e^2 \eta D_u}{cn_r \epsilon_0 m_0^2 v_d} \frac{|P_{cv}|^2}{E_u} \frac{\xi}{\Gamma_o} (2P_u - 1) = K_u (2P_u - 1) \quad (8)$$

$$g_{es} = \frac{2\pi e^2 \eta D_e}{cn_r \epsilon_0 m_0^2 v_d} \frac{|P_{cv}|^2}{E_e} \frac{\xi}{\Gamma_o} (2P_e - 1) = K_e (2P_e - 1) \quad (9)$$

$$g_{gs} = \frac{2\pi e^2 \eta D_g}{cn_r \epsilon_0 m_0^2 v_d} \frac{|P_{cv}|^2}{E_g} \frac{\xi}{\Gamma_o} (2P_g - 1) = K_g (2P_g - 1) \quad (10)$$

$P_u$ ,  $P_e$ ,  $P_g$  are occupation probability of CS, ES and GS state, respectively.

$$P_u = \frac{N_u}{2D_u N_D} \quad (11)$$

$$P_e = \frac{N_e}{2D_e N_D} \quad (12)$$

$$P_g = \frac{N_g}{2D_g N_D} \quad (13)$$

Also, we can write the relationship between relaxation times and escape times. In equations below  $T_{eg}$ ,  $T_{ug}$ ,  $T_{ue}$ ,  $T_{wu}$  are relaxation times and  $T_{eu}$ ,  $T_{gu}$ ,  $T_{ge}$ ,  $T_{uw}$  are escape times.

$$T_{gu} = T_{ug} \left( \frac{D_g}{D_u} \right) \exp \left( \frac{E_u - E_g}{K_B T} \right) \quad (14)$$

$$T_{ge} = T_{eg} \left( \frac{D_g}{D_e} \right) \exp \left( \frac{E_e - E_g}{K_B T} \right) \quad (15)$$

$$T_{eu} = T_{ue} \left( \frac{D_e}{D_u} \right) \exp \left( \frac{E_u - E_e}{K_B T} \right) \quad (16)$$

Escape times and relaxation times have an exponential relation with each other. Relaxation times in experimental model varies with equations below:

$$T_{ug} = \frac{T_{ugo}}{1 - P_g} \quad (17)$$

$$T_{eg} = \frac{T_{ego}}{1 - P_e} \quad (18)$$

$$T_{ue} = \frac{T_{ueo}}{1 - P_e} \quad (19)$$

In these equations  $|P_{cv}|$  is absolute transition matrix element,  $\xi$  is coverage factor,  $\Gamma_o$  is non-homogeneous broadening factor,

$v_d$  is QD volume,  $N_D$  is QD volume density,  $\epsilon_{us}$ ,  $\epsilon_{es}$ ,  $\epsilon_{gs}$  are gain compression. Some parameters are mentioned in Table.1.

### III. Results and Tables

In this section, numerical results are presented. **Fig.2** is diagram of output power for ground state as a function of bias current for three various values of inhomogeneous broadening factor. The first value is less than experimental one, the second is the same as real value used in experimental model [xxii] and the last one is more than experimental value. We have chosen these values in this figure and other figures to compare numerical result to optimize it better. Simulation shows that threshold intensity to start lasing from ground state is very low and it would be constant approximately with increasing inhomogeneous broadening factor. However, it is clear that with increasing inhomogeneous broadening factor we will have less output power for GS. So to have a much more output power it is better to decrease inhomogeneous broadening factor. As well as, with enhancing inhomogeneous broadening factor, output power will be saturated in lower current.

**Fig.3** is a diagram of output power for excited state as a function of bias current for the three various values of inhomogeneous broadening factor. As we have said, values for Fig.2 is the same as diagram of output power for ground state as a function of bias current for three various values of inhomogeneous broadening factor are the same as we used for GS. With considering diagram 3, whatever Fig.2 is diagram of output power for ground state as a function of bias current for three various values of inhomogeneous broadening factor is increased, threshold bias current to begin lasing is declined for ES. In addition, with augmentation inhomogeneous broadening factor output power for ES will decrease in saturated values. It means output power will be saturated in lower bias current with enhancement of inhomogeneous broadening factor with lower output power for ES.

**Fig.4** displays output power for CS as a function of bias current for three values of inhomogeneous broadening factor. As you see, it declares that lasing from CS start from an almost high bias current. In other words, if we want to have lasing from CS, we have to increase bias current about 15 (A) with considering experimental value of inhomogeneous broadening factor (the second one). This is the meaning of three state lasing of InGaAs/GaAs QD laser. It has clearly shown we have more output power with less inhomogeneous broadening factor, however, it is not rational to work with emitting laser from CS since its high bias current. Finally it will be saturated like prior diagram for GS and ES, but with a high bias current (more than 25 (A)). Now, here we would like to discuss optical gain and its dependence to inhomogeneous broadening factor for each state separately to figure out best values to optimize InGaAs/GaAs QD laser. At first, consider **Fig.5** that is the diagram of optical gain for ground state as a function of bias current. It is clear that optical gain is low for QD lasers and it is one of characteristics

of them. It declares that with enhancement of inhomogeneous broadening factor optical gain will be saturated in higher current.

Parameter	Value
Transition energy from GS, $E_g$	1050 meV
Transition energy from ES, $E_e$	1090 meV
Transition energy from CS, $E_u$	1140 meV
Active region length, $L_{ca}$	1000 $\mu m$
Reflectivity of mirrors	$R_1=R_2=0.3$
Degeneracy of GS, $D_g$	1
Degeneracy of ES, $D_e$	3
Degeneracy of CS, $D_u$	10
Total optical confinement factor, $\Gamma$	0.1
Spontaneous emission coupling factor, $\beta$	$10^{-7}$
Velocity group, $V_g$	$8.571 \times 10^7$ m/s
Carrier injection rate, $\eta_i$	0.9
Spontaneous recombination time, $T_{sp}$	500 ps
Initial relaxation time from CS to GS, $T_{ugo}$	2 ps
Initial relaxation time from ES to GS, $T_{ego}$	6 ps
Initial relaxation time from CS to ES, $T_{ueo}$	2 ps

**Table.1.** Constant values used in simulations

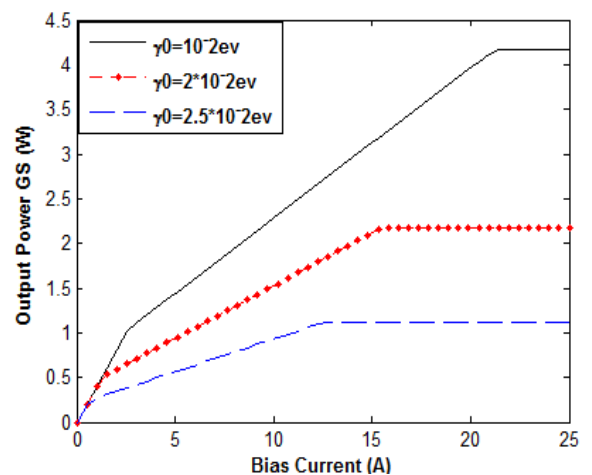


**Fig.2.** Output power for ground state as a function of bias current for various inhomogeneous broadening values

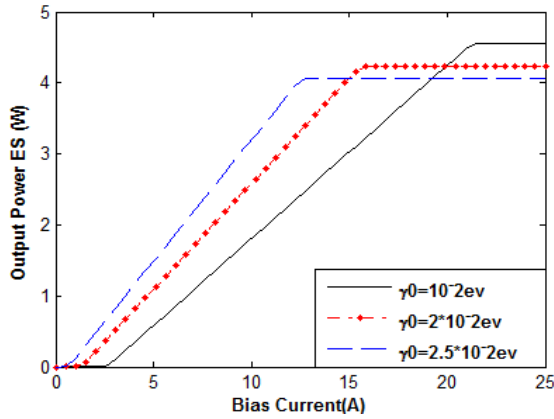


**Fig.3.** Output power for excited state as a function of bias current for various inhomogeneous broadening values

As you see optical gain will saturate with the same value for all these three values of inhomogeneous broadening factor.

In **Fig.6** we have calculated the same numerical values for excited state. Just like the same one for ground state, optical gain is not so high and it would be saturated at a parallel quantity for all three values of inhomogeneous broadening factor. At first with increasing bias current than zero, there is a negative optical gain, but with increasing more it will become positive that means lasing has started efficiently. More with increasing bias current it saturation will appear at the same value for all three amount of inhomogeneous broadening factor. It is shown clearly current should be so more for ES in comparison with the same diagram for GS.

**Fig.7** is a diagram of optical gain for lasing from CS as function of bias current. It is significantly that with comparison between this diagram and Fig.6, we can quickly figure out bias current for CS is much more higher than ES and we cannot have positive gain for CS in a low amount of current. In addition, it is visible in CS with increasing inhomogeneous broadening factor optical gain will be saturated in lower current. It means that saturation and inhomogeneous broadening factor have a contrary behaviour with each other. However, like two last diagrams for GS and ES, optical gain would have a one value after saturation for all three inhomogeneous broadening factor values.

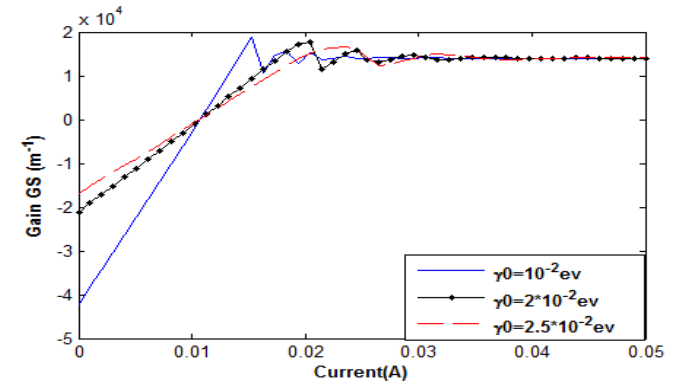


**Fig.5.** Optical gain for ground state as a function of bias current for various inhomogeneous broadening values

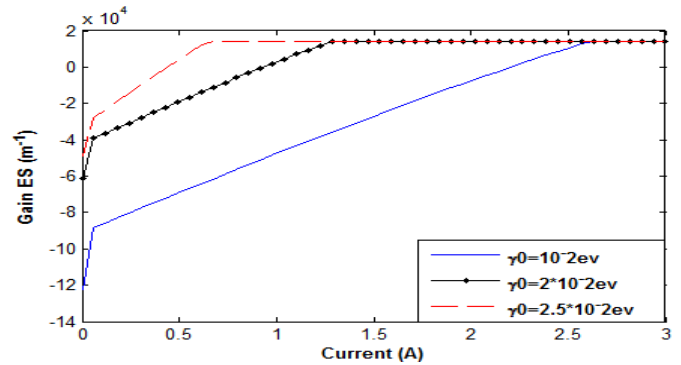


**Fig.6.** Optical gain for excited state as a function of bias current for various inhomogeneous broadening values

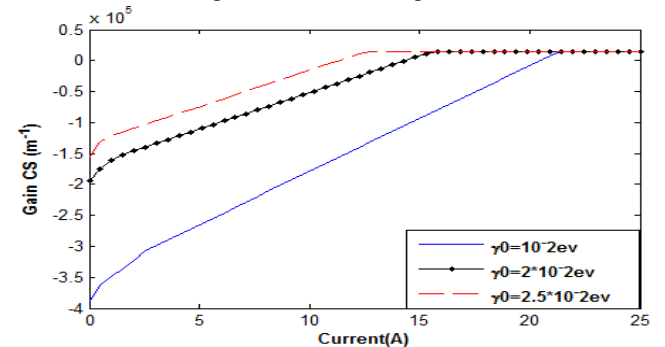


**Fig.7.** Optical gain for upper continuum state as a function of bias current for various inhomogeneous broadening values

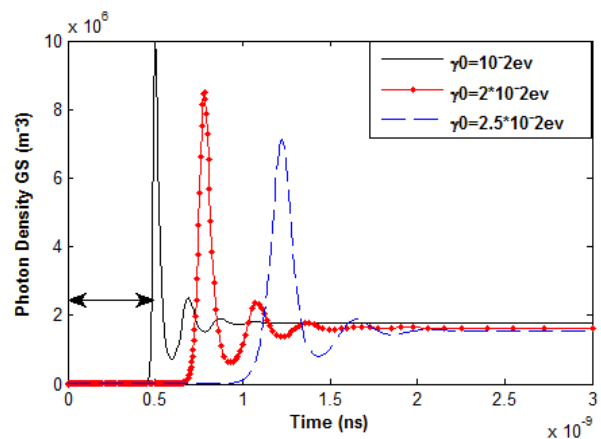


**Fig.8.** Photon density for ground state as a function of time for various inhomogeneous broadening values

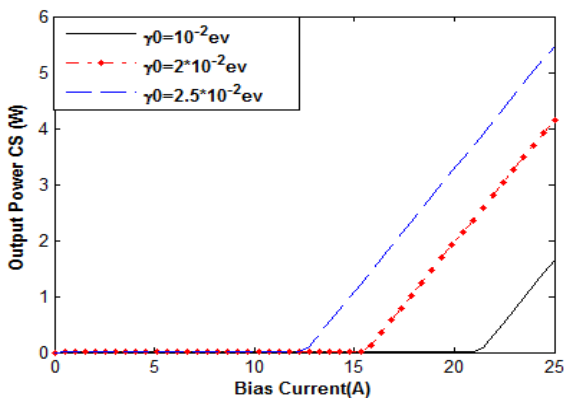


**Fig.4.** Output power for upper continuum state as a function of bias current for various inhomogeneous broadening values



Finally, we have investigated photon density for ground state as a function of time in **Fig.8**. This useful figure demonstrates that with intensification of inhomogeneous broadening values for InGaAs/GaAs (QD) lasers the result will be less photon density in saturation state for GS. Furthermore, turn on delay as an important significant is pointed in figure 8, we can recognize that with increasing inhomogeneous broadening factor, turn on delay will increase too. This is significant to decline turn on delay, with comparison less and more values of inhomogeneous broadening

with one is used in real model, for optimizing we is better to decrease inhomogeneous broadening factor to have less turn on delay.

#### IV. Conclusion

With the computed results, we have found that intrinsically, with increasing inhomogeneous broadening factor, output power for ground state will decrease with a constant threshold current for any value, but threshold current to start lasing for excited state will increase. Due to inhomogeneous broadening certain deductions of QDs do not participate in laser transition and will add to parasitic remix. Also with increasing inhomogeneous broadening saturated gain decreases.

#### References

- i. I. P. Marko, N. F. Masse, S. J. Sweeney, A. D. Andreev, A. R+. Adams, N. Hatori, and M. Sugawara, "Carrier transport and recombination in p-doped and intrinsic 1.3  $\mu\text{m}$  InAs/GaAs quantum-dot lasers," *Appl. Phys. Lett.*, vol. 87, no. 21, pp. 211114-1–211114-3, Nov. 2005.
- ii. P. M. Snowton, I. C. Sandall, H. Y. Liu, and M. Hopkinson, "Gain in p-doped quantum dot lasers," *J. Appl. Phys.*, vol. 101, no. 1, pp. 013107-1–013107-7, Jan. 2007.
- iii. O. B. Shchekin and D. G. Deppe, "The role of p-type doping and the density of states on the modulation response of quantum dot lasers," *Appl. Phys. Lett.*, vol. 80, no. 15, pp. 2758–2760, Apr. 2002.
- iv. K. Mukai, Y. Nakata, K. Otsubo, M. Sugawara, N. Yokoyama, and H. Ishikawa, "1.3- $\mu\text{m}$  CW lasing characteristics of self-assembled InGaAs-GaAs quantum dots," *IEEE J. Quantum Electron.*, vol. 36, no. 4, pp. 472–478, Apr. 2000.
- v. M. Vasileiadis, D. Alexandropoulos, M. J. Adams, H. Simos, and D. Syvridis, "Potential of InGaAs/GaAs quantum dots for applications in vertical cavity semiconductor optical amplifiers," *IEEE J. Sel. Topics Quantum Electron.*, vol. 14, no. 4, pp. 1180–1187, Jul./Aug. 2008.
- vi. V. Ahmadi and M. H. Yavari, "Analysis of carrier and photon dynamics effects on the modulation behavior of self assembled quantum dot lasers," *IEEE Int. Conf. Transparent Opt. Netw. (ICTON)*, Jun. 2008, vol. 2, pp. 137–140.
- vii. M. H. Yavari, V. Ahmadi, and P. Rafiee, "Modulation characteristics of self-assembled InAs-GaAs quantum dot laser considering phonon bottleneck, carrier relaxation and homogeneous broadening," *IEEE Int. Conf. Transparent Opt. Netw. (ICTON)*, Dec. 2009, pp. 1–4.
- viii. N. Ledentsov, D. Bimberg, V. M. Ustinov, Zh. I. Alferov, and J. A. Lott, "Quantum dots for VCSEL applications at  $\lambda = 1.3 \mu\text{m}$ ," *Physica E*, vol. 13, pp. 871–875, 2002.
- viii. R. P. Sarzala, "Modeling of the threshold operation of 1.3- $\mu\text{m}$  GaAs-based oxide-confined (InGa) As-GaAs quantum-dot vertical-cavity surface-emitting lasers," *IEEE J. Quantum Electron.*, vol. 40, no. 6, pp. 629–639, Jun. 2004.
- ix. L. Asryan and R. Suris, "Inhomogeneous line broadening and the threshold current density of a semiconductor quantum dot laser," *Semicond. Sci. Technol.*, vol. 11, no. 4, pp. 554–567, 1996.
- x. H. Dery and G. Eisenstein, "The impact of energy band diagram and inhomogeneous broadening on the optical differential gain in nanostructure lasers," *IEEE J. Quantum Electron.*, vol. 41, no. 1, pp. 26–35, Jan. 2005.
- xi. M. Sugawara, K. Mukai, Y. Nakata, H. Ishikawa, and A. Sakamoto, "Effect of homogeneous broadening of optical gain on lasing spectra in self-assembled InxGa1-xAs /GaAs quantum dot lasers," *Phys. Rev. B*, vol. 61, pp. 7595–7603, 2000.
- xii. A. Sakamoto and M. Sugawara, "Theoretical calculation of lasing spectra of quantum-dot lasers: Effect of homogeneous broadening of optical gain," *IEEE Photon Technol. Lett.*, vol. 12, no. 2, pp. 107–109, Feb. 2000.
- xiii. M. Sugawara, N. Hatori, H. Ebe, and M. Ishida, "Modeling room-temperature lasing spectra of 1.3- $\mu\text{m}$  self-assembled InAs/GaAs quantum-dot lasers: Homogeneous broadening of optical gain under current injection," *J. Appl. Phys.*, vol. 97, pp. 43523–43527, 2005.
- xiv. D. Greedy and G. Eisenstein, "Carrier dynamics in tunneling injection quantum dot lasers," *IEEE J. Quantum Electron.*, vol. 46, no. 11, pp. 1611–1618, Nov. 2010.
- xv. A. K. Ludge, M. J. P. Bormann, E. Malic, P. Hovel, M. Kuntz, D. Bimberg, Knorr, and E. Scholl, "Turn-on dynamics and modulation response in semiconductor quantum dot lasers," *Phys. Rev. B*, vol. 78, pp. 35316–35327, 2008.
- xvi. P. Bhattacharya, S. Ghosh, S. Pradhan, J. Singh, Z. Wu, J. Urayama, K. Kim, T. Theodore, and B. Norris, "Carrier dynamics and high-speed modulation properties of tunnel injection InGaAs-GaAs quantum-dot lasers," *IEEE J. Quantum Electron.*, vol. 39, no. 8, pp. 952–962, Aug. 2003.
- xvii. D. G. Deppe, H. Huang, and O. B. Shchekin, "Modulation characteristics of quantum-dot lasers: The influence of p-type doping and electronic density of states on obtaining high speed," *IEEE J. Quantum Electron.*, vol. 38, no. 12, pp. 1587–1593, Dec. 2002.
- xviii. D. G. Deppe and H. Huang, "Fermi's golden rule, nonequilibrium electron capture from the wetting layer, and the modulation response in p-doped quantum-dot lasers," *IEEE J. Quantum Electron.*, vol. 42, no. 3, pp. 324–330, Mar. 2006.
- xix. D. G. Deppe and D. L. Huffaker, "Quantum dimensionality, entropy, and the modulation response of quantum dot lasers," *Appl. Phys. Lett.*, vol. 77, pp. 3325–3327, 2000.
- xx. C. Z. Tong, D. W. Xu, and S. F. Yoon, "Carrier relaxation and modulation response of 1.3  $\mu\text{m}$  InAs-GaAs quantum dot lasers," *J. Lightw. Technol.*, vol. 27, pp. 5442–5450, 2009.
- xxi. C. L. Tan, Y. Wang, H. S. Djie I, B. S. Ooi, "The role of optical gain broadening in the ultrabroadband InGaAs/GaAs interband quantum-dot laser," *Computational Materials Science* 44 (2008) 167–173